applied sciences

MDPI

Brief Report

Saturation Effect on the Coherency Loss of Spatially Varying Vertical Ground Motions

Erlei Yao, Zhaowei Yang, Yu Rao, Xiuli Ding, Zhifang Liu, Xiujie Wang, Wenbo Liu and Weichao Li *

Key Laboratory of Geotechnical Mechanics and Engineering of the Ministry of Water, Changjiang River Scientific Research Institute, Wuhan 430010, China
* Correspondence: liwc0905@mail.crsri.cn

Abstract: The effect of the influence regularity of site saturation and water level on the coherency loss between spatially varying earthquake ground motions (SVEGMs) in a vertical direction is not yet clear. Therefore, taking an onshore-offshore site as an example, the influence regularity of site saturation and water level on the coherency loss of SVEGMs in a vertical direction was studied, in which the saturation degree of the whole site (SD), the groundwater level (GWL), and the thickness of the surface water layer (WLT) were considered. Under each case mentioned above, a large number of vertical in-plane SVEGMs were synthesized and then correspondingly, the mean lagged coherency loss and phase angle of coherence function were obtained, and a series of comparisons were carried out to shed light on the varying trend of the value of lagged coherency loss and phase angle, with predefined parameters. The results showed that SD, GWL, and WLT possess significant effects on the varying trend of the coherence function of vertical SVEGMs.

Keywords: coherency loss; spatially varying earthquake ground motions; water saturation; water layer; influence regularity

check for updates

Citation: Yao, E.; Yang, Z.; Rao, Y.; Ding, X.; Liu, Z.; Wang, X.; Liu, W.; Li, W. Saturation Effect on the Coherency Loss of Spatially Varying Vertical Ground Motions. *Appl. Sci.* **2023**, *13*, 4302. https://doi.org/10.3390/app13074302

Academic Editor: Jong Wan Hu

Received: 20 February 2023
Revised: 25 March 2023
Accepted: 27 March 2023
Published: 28 March 2023

Copyright: © 2023 by the authors. Licensee MDPI, Basel, Switzerland. This article is an open access article distributed under the terms and conditions of the Creative Commons Attribution (CC BY) license (https://creativecommons.org/licenses/by/4.0/).

1. Introduction

The simulation technology of SVEGMs greatly facilitates the seismic study of extended structures, e.g., tunnels, dams, and bridges [1–6]. For the seismic analysis and earthquake-resistant design of offshore platforms and sea-crossing bridges etc., onshore earthquake records or artificial waves are usually used as inputs due to the lack of offshore records and seismic motions simulation methods applicable to offshore sites. However, the pore-water saturation of the soil layer and the seawater layer may strongly affect the amplitudes of vertical in-plane motions [7]. Thus, many researchers have studied the influence of the surface water layer, or site saturation, on the ground motions and proposed several methods to generate offshore SVEGMs. Bureau [8] and Feng [9] indicated that the depth of the seawater is significant to the offshore vertical response. Crouse and Quilter [10] explained why the water layer can greatly suppress the vertical site response at the resonant frequencies of P-waves in the water layer. Boore and Smith [11] found that the water layer does not have a significant effect on the horizontal components of motion, but will produce a significant reduction in the vertical components of motion near the resonant frequencies of the P-waves in the water layer. Diao et al. [12] conducted a theoretical analysis of the effect of seawater on incident plane P-and SV-waves at the ocean bottom. Li et al. [13] derived an offshore transfer function model and then developed a method simulate seafloor seismic motions. Considering the effect of the soft soil layer and soil saturation on site transfer function, Fan et al. [7] presented a new method to study the effect of the seawater layer on vertical in-plane motions. Shi et al. [14] proposed a new method of modeling spatially varying ground motion due to the ice-seawater layer, where the effects of water saturation on vertical ground motion were considered. Zhang et al. [15] presented a comprehensive and rational approach of synthesizing three directional spatially correlated earthquake ground motions, which took into consideration the effect of Poisson's ratio of

water saturation on soil. Li et al. [16] established a modeling and simulation method for three-dimensional spatially correlated ground motion at multiple onshore and offshore sites in which hydrodynamics and one-dimensional wave propagation theory were utilized to construct the transfer function. Liu et al. [17] reported a simulation method of spatially variable seismic underground motions in saturated double-phase media with overlying water excited by an SV-wave. Considering a saturated alluvial valley site, He et al. [18] developed an effective simulation method for multiple-station spatially correlated ground motions on both the bedrock and the surface. The achievements in this scientific field have contributed to the seismic analysis or earthquake-resistant design of many important large scale offshore structures (e.g., Unocal Platform Irene, Southern California, USA; Hong Kong-Zhuhai-Macao Bridge, Southern Guangdong, China). However, the influence regularity study of the saturation and the surface water layer on the coherency loss between vertical SVEGMs is not included in the abovementioned works and has not received wide attention, and the understanding level of this effect is low. Revealing the effect of the influence regularity of saturation and the surface water layer on the coherency loss function can strengthen the understanding of hazards resulting from SVEGMs, and, for a certain project, the influence regularity study of saturation and surface water layer can contribute to summarizing the coherency loss model. It can then facilitate the fast generation of numerous SVEGMs, generating significant meaning for the three-dimensional seismic analysis, reliability analysis, and earthquake-resistant design of large off-coast structures.

Moreover, to facilitate the seismic analysis and earthquake-resistant design of onshore-offshore extended structures which are usually located in sites with irregular topography, many have paid attention to the effect of irregular topography [19–21] and site conditions [22–25] on the coherency loss of SVEGMs. In the works mentioned above, however, the influence of water saturation, water level, or surface water layer were scarcely considered, and at the same time, the influence regularity of water saturation or water level on the coherency loss between SVEGMs is not clear.

Therefore, taking an onshore-offshore site as example, the influence regularity of site saturation and water level on the coherency loss of vertical SVEGMs was studied in the present paper, where the SD of the whole site, GWL, and WLT were taken into account. Under each circumstance mentioned above, a large number of vertical in-plane SVEGMs were synthesized based on the one-dimension wave propagation theory [26], and the mean lagged coherency loss and phase angle were estimated; then, the varying trend of lagged coherency loss and phase angle with SD, GWL, and WLT was obtained.

2. Materials and Methods

The transfer function in the one-dimension wave propagation theory [26] was utilized to describe the amplification and filtering effects of soil on the incident wave. The formulas for estimating the P-wave velocity of a porous medium, proposed by Yang and Sato [27], were employed to represent the effect of water saturation on the site amplification. The establishment method of the dynamic-stiffness matrix of the water layer, derived by Li et al. [13], was adopted in the study case with WLT to facilitate the establishment of the total dynamic-stiffness matrix of site under water. Based on the methods or parameters mentioned above, the transfer function of target site considering the saturation, or surface water layer, can be established. Then, the auto/cross-power spectral density function (PSDF) on site surface can be derived [4,6]:

$$S_{jj}(\omega) = \left|H_j(i\omega)\right|^2 S_g(\omega) \quad j = 1, 2, \ldots n, \tag{1}$$

and

$$S_{jk}(i\omega) = H_j(i\omega) H_k^{\Theta}(i\omega) S_g(\omega) \gamma_{j'k'}(d_{j'k'}, i\omega) \quad j, k = 1, 2, \ldots n, \tag{2}$$

respectively, where H_j and H_k are the transfer functions at simulation points j and k, respectively; superscript 'Θ' denotes the complex conjugate; $S_g(\omega)$ is the ground motion PSDF at

the base rock; $\gamma_{j'k'}(d_{j'k'}, i\omega)$ is the coherency loss function between bedrock motions, which is related to the separation distance $d_{j'k'}$ and ω.

By using the classical spectral representation method [19] in combination with Jennings window, non-stationary SVEGMs can be generated by

$$f_j(t) = 2a(t)\sum_{x=1}^{n}\sum_{y=1}^{N}\left|U_{jx}(\omega_y)\right|\sqrt{\Delta\omega}\cos[\omega_y t - \theta_{jx}(\omega_y) + \Phi_{xy}] \quad j = 1, 2, \ldots n \tag{3}$$

$$\omega_y = y\Delta\omega \quad y = 1, 2, \ldots N \tag{4}$$

$$\Delta\omega = \frac{\omega_u}{N} \tag{5}$$

$$\theta_{jx}(\omega_y) = \tan^{-1}\left(\frac{\mathrm{Im}[U_{jx}(\omega_y)]}{\mathrm{Re}[U_{jx}(\omega_y)]}\right) \tag{6}$$

with $\Delta\omega$ denoting the bandwidth and N the number of frequency intervals. ω_u represents an upper cut-off frequency beyond which the elements of the power spectral density matrix (PSDM) may be assumed to be zero for any time instant. $U_{jx}(\omega_y, t)$ is an element of the matrix obtained through the decomposition of PSDM. Φ_{xy} is a random phase angle uniformly distributed in [0, 2π]. $a(t)$ is a modulating function in time.

The filtered Tajimi–Kanai model [28] is utilized to describe the PSDF on the bedrock:

$$S_g(\omega) = \frac{\omega^4}{\left(\omega_f^2 - \omega^2\right)^2 + \left(2\omega_f\omega\zeta_f\right)^2} \times \frac{\omega_g^4 + 4\zeta_g^2\omega_g^2\omega^2}{\left(\omega_g^2 - \omega^2\right)^2 + 4\zeta_g^2\omega_g^2\omega^2}S_0 \tag{7}$$

where ω_g and ζ_g are the central frequency and damping ratio of the Tajimi–Kanai PSDF; ω_f and ζ_f are the central frequency and damping ratio of the high pass filter; and S_0 is the scaling factor. According to Bi and Hao [19], $\omega_g = 10\pi\mathrm{rad/s}$, $\zeta_g = 0.6$, $\omega_f = 0.5\pi$, $\zeta_f = 0.6$ and $S_0 = 0.0034\ \mathrm{m^2/s^3}$. These parameters correspond to a ground motion time history with a duration 20 s and peak ground acceleration (PGA) 0.2 g. The Sobczyk model [29] is selected to describe the coherency loss between the ground motions at points j' and k' as follows:

$$\gamma_{j'k'}(i\omega) = \exp(-\beta\omega d_{j'k'}^2/Ve)\cdot\exp(-i\omega d_{j'k'}\cos\alpha/Ve) \quad j', k' = 1', 2', 3' \tag{8}$$

where β = 0.0005 is used herein [29]; α is the incident angle of the incoming wave to the site; *Ve* is the apparent velocity which is set to 1800 m/s, according to the bedrock property and the specified incident angle. The Jennings window is employed to model the temporal non-stationarity of simulated ground motions, which has the following form

$$a(t) = \begin{cases} (t/t_1)^2 & t < t_1 \\ 1 & t_1 \le t < t_2 \\ \exp[-c(t - t_2)] & t \ge t_2 \end{cases} \tag{9}$$

where t_1, t_2, and c are set to 6, 10, and 0.5, respectively.

3. Numerical Example

In this section, the information from the study cases and the parametric study conducted herein is introduced first, and then relevant results are analyzed. Three cases (numbered as case-1, case-2, and case-3) were considered in this study: case-1 evaluates the parametric study with varying SD, case-2 examines the varying GWL, and case-3 investigates the varying WLT. Based on these three cases, the effect of SD, GWL, and WLT on the coherency loss between vertical SVEGMs was investigated. Figure 1 shows the diagram of the study cases performed, where ρ is medium density, μ the Poisson's ratio of the soil

skeleton, G is the shear modulus, ξ is the damping ratio, n is the porosity, P is the absolute fluid pressure, Kw is the bulk modulus of water, and S_r is the saturation degree. Besides, herein, the bulk modulus of the solid skeleton is $K_b = 8.67 \times 10^7$ Pa; the bulk modulus of solid grains is $K_s = 3.6 \times 10^{10}$ Pa. Specific cases involved are summarized in Table 1, and fundamental information of simulated seismic motions is shown in Table 2. Simulation points, j and k, with a horizontal spacing distance of 100 m, are set. For every single parameter in each case, 1000 simulations were performed to calculate the mean lagged coherency loss and phase angle of the coherence function between the ground motions. Note that the case with 95% SD in case-1 is equivalent to that with GWL = 0 m in case-2, and the case with GWL = 30 m in case-2 is equivalent to that with WLT = 0 m in case-3.

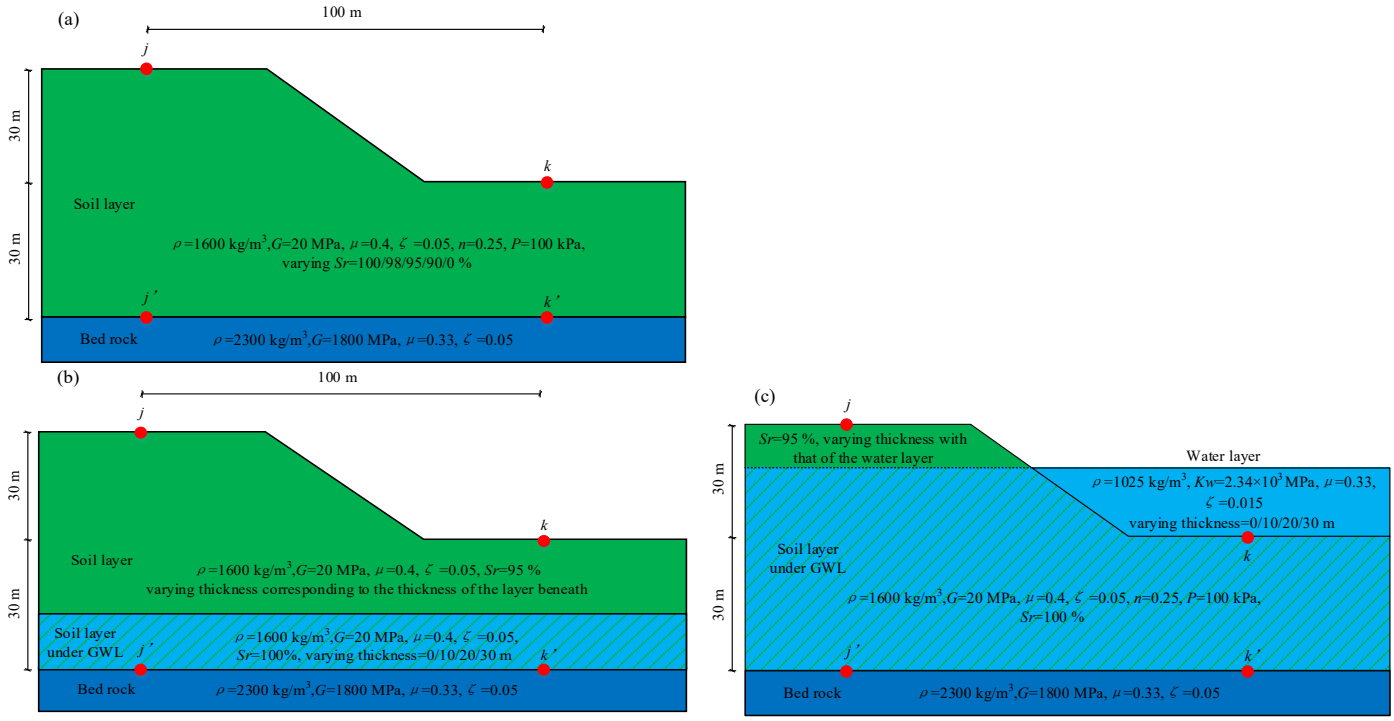


Figure 1. Diagrams of site conditions for: (**a**) the case with varying SD; (**b**) the case with varying GWL; (**c**) the case with varying WLT at point k (not to scale).

Table 1. Study cases performed.

No. of Case	Soil SD/%	GWL for the Whole Site/m	WLT at Point k/m
Case-1 (the case with varying SD)	100/98/95/90/0	-	-
Case-2 (the case with varying GWL)	above GWL: 95 under GWL: 100	0/10/20/30	-
Case-3 (the case with varying WLT at point k)	above water layer surface: 95 under water layer surface: 100	30 40 50 60	0 10 20 30

Table 2. Fundamental information of simulated seismic motions.

Incident Angle	Total Duration	Upper Cut-Off Frequency	PGA	Sampling Frequency	No. of Sampling Points
60°	20 s	25 Hz	0.2 g	100 Hz	2048

The amplitudes of the transfer functions for all cases are shown in Figure 2. From Figure 2a, it can be found that as the SD increases, the amplitude of the transfer function decreases, and the predominant frequency shifts toward the high frequency end; especially when the SD increases from 98% to 100%, the amplitude decreases sharply. This is consistent with the results of Yang and Sato [27], which verifies the reliability of the results in this paper, to some extent. Moreover, by observing the transfer functions in Figure 2b,c it can be found that: (i) for site j, the vertical motion is amplified until the site is fully saturated; (ii) for site k, when the water table is under the site surface, the vertical motion is amplified; in contrast, when there is a water layer on the surface (the water table is above the surface), the vertical motion is suppressed at a certain frequency point. Therefore, the state of full saturation (i.e., SD = 100% in case-1, the GWL = 30 m for site k in case-2, or the WLT = 0 m for site k in case-3) is the critical state of amplification and suppression. In other words, when the site is incompletely saturated, amplification can be observed; when the site is fully saturated, vertical motion would be slightly suppressed; and when the site is fully saturated and under a water layer, the vertical wave would be significantly suppressed. Therefore, the state of saturation is the turning point. The resonant frequency of P-wave, f_n, in the water layer can be defined as [13]

$$f_n = n\frac{c_p^{*w}}{4d\sin\theta_p^w}, \quad n = 1, 3, 5\ldots \tag{10}$$

in which d denotes the depth of water layer, c_p^{*w} the wave speed of the P-wave in the water layer, and θ_p^w the inclined angle of the P-wave. For the numerical example in the present paper, when d = 20 and 30 m, the corresponding first-order resonant frequencies of the water layer are 21.81 and 14.54 Hz, respectively. Then, from Figure 2c, it can be found that the transfer functions are suppressed near 21.81 and 14.54 Hz, respectively, which verifies the validity of the results of this paper, to some extent again.

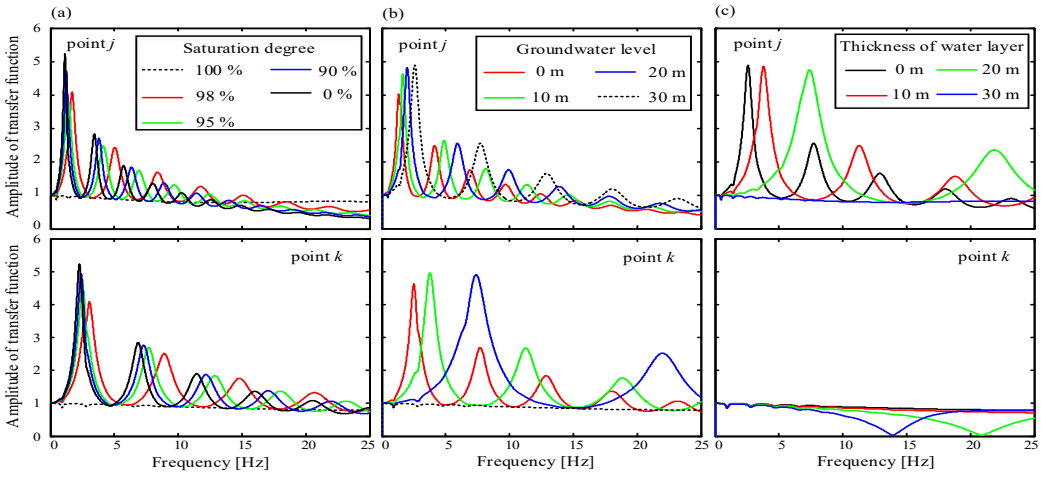


Figure 2. Amplitude of transfer function for varying: (**a**) SD; (**b**) GWL; (**c**) WLT.

Figure 3 gives the mean lagged coherency loss and corresponding mean phase angle of the coherence function for the generated vertical in-plane motions, where the corresponding modulus of the spectral ratio between sites j and k are also given (here, spectral ratio is defined as the ratio between the transfer functions at sites j and k, and the peaks and troughs of the amplitude curve of the spectral ratio reflect the difference between the transfer function between sites j and k). As can be seen, the troughs of each lagged coherency loss function are directly related to the peaks of the corresponding spectral ratios, and due to the topography effect, the amplitude of the coherency function exhibits additional loss, which is consistent with previous results [25]. As the SD increases, the lagged coherency loss for vertical seismic motions gradually approaches that for bedrock motions, indicating

that the existence of groundwater can make up the extra lagged coherency loss due to the topography effect. The higher the SD, the higher the P-wave velocity [27] in the medium and the stiffness of the site in the vertical direction; thus, the amplitude of the transfer function for sites j and k tends to be simultaneously lower, and the spectral ratio may decrease. Note that when the site is fully saturated, both the transfer functions at sites j and k are approximately 1 or slightly lower than 1, indicating that the amplification and filtering effect of the site on the vertical motion almost vanish, and thus, at this time, the difference between the seismic waves at sites j and k is mild, and the extra coherency loss is very small. In other words, the higher the SD, the smaller the extra lagged coherency loss due to the topography effect.

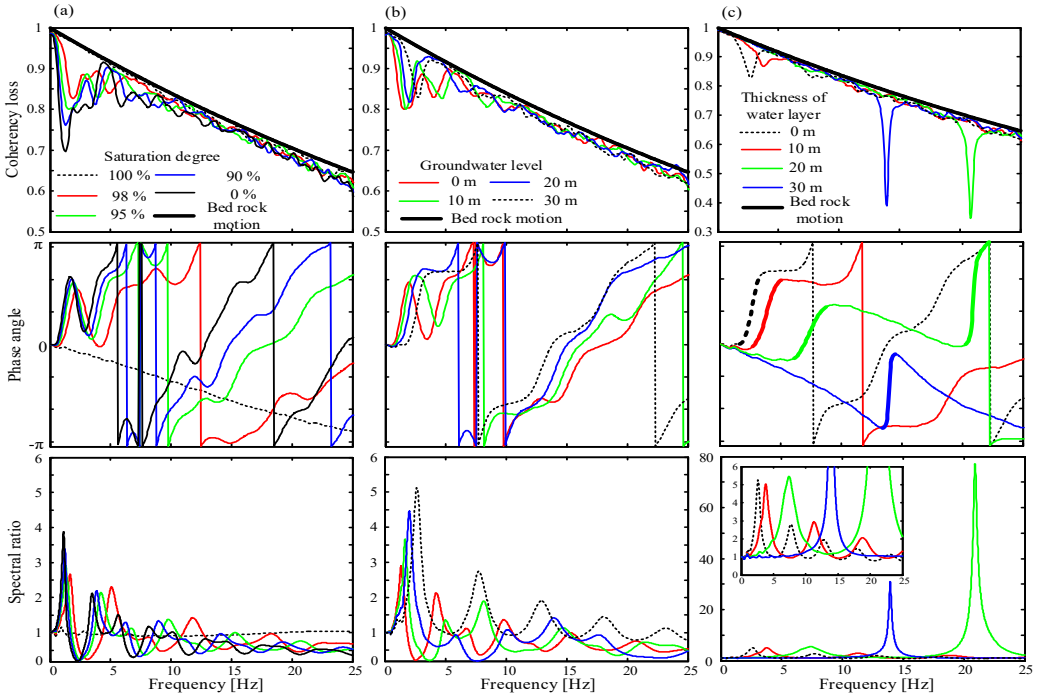


Figure 3. Coherence functions and relevant spectral ratios for varying: (**a**) site SD; (**b**) GWL; (**c**) WLT.

When it comes to water level, the authors analyze relevant results by combining case-2 and case-3 herein. The extra loss of the lagged coherence function decreases with increasing water levels, except for the values corresponding to extremely sharp peaks (corresponding to the P-wave resonant frequency of the water layer) of the spectral ratio curve. The existence of a fully saturated soil layer dramatically decreases the propagation time of the vertical wave inner site (c_p = 2224.7 m/s in fully saturated soil layer, while c_p = 282.79 m/s in a soil layer with SD = 95%) and then the time delay between sites j and k, causing the superposition modes of the wave at sites j and k to be similar, and as thickness of fully saturated soil layer increases, the time delay would become lower and lower. Therefore, to a certain extent, the extra coherency loss due to irregular topography can be made up by an underlying fully saturated soil layer, and this phenomenon tends to be more remarkable as water table becomes higher and higher. At the frequencies where the vertical motion is suppressed significantly by the surface water layer, the value of coherency loss is extremely low. This is because around the frequencies where vertical motion is suppressed significantly by the surface water layer, the frequency content of the motions at j and k is extremely different. Coherency loss function only evaluates the difference between motions. Therefore, the larger the difference between the frequency content of motions, the lower the coherency loss.

As to the phase angle of the coherence function, there is always a remarkable change (e.g., local bold lines shown in Figure 3c) showing up around the frequency point corre-

sponding to each peak of the spectral ratio curve, indicating that when the amplitudes of transfer functions at sites *j* and *k* differ greatly, the phase angle of the coherency function exhibits significant variation. Besides, the curves for the phase angle also gradually shift towards the high frequency end as spectral ratio varies with increasing SD, GWL, and WLT. All of the above mentioned indicate that the phase angle of the coherency function is also directly related to the spectral ratio.

4. Conclusions

In the present paper, the effect of the influence regularity of the site saturation degree, the height of the groundwater level, and the thickness of the surface water layer on the coherency loss of vertical SVEGMs was studied based on the 1D wave propagation theory, the dynamic-stiffness matrix of the surface water layer, and the effect of site saturation on the amplification of seismic wave. The results showed that (i) generally, the state of full saturation is the critical state determining whether the vertical motion is amplified or suppressed, and natural frequencies of spectral ratios increase as SD, GWL, and WLT increase; (ii) as the site saturation degree and water table increases, the value of the lagged coherency loss for the vertical seismic motions gradually increases (i.e., gradually approaches that for bedrock motion), and at the frequencies where vertical motion is suppressed significantly by the surface water layer, the value of coherency loss is extremely low; (iii) there is always a remarkable change of phase angle showing up around the frequency point corresponding to each peak of spectral ratio curve, and the curves of phase angle gradually shift towards high frequency end as spectral ratio varies with increasing SD, GWL, and WLT. However, the present results are based on a local homogeneous soil site, and random soil properties are not considered, which will be taken into consideration in future work.

Author Contributions: Conceptualization, E.Y.; methodology, E.Y.; software, Z.Y.; validation, Z.Y. and Y.R.; formal analysis, W.L. (Weichao Li); investigation, W.L. (Weichao Li); resources, Y.R.; data curation, X.W.; writing—original draft preparation, E.Y.; writing—review and editing, Z.L.; visualization, W.L. (Wenbo Liu); supervision, X.D.; project administration, W.L. (Weichao Li); funding acquisition, E.Y. All authors have read and agreed to the published version of the manuscript.

Funding: This study was financially supported by the Knowledge Innovation Program of Wuhan-Shuguang (No. 2022010801020242), the National Natural Science Foundation of China (Nos. 51908236, 51978304, 51778260, and 52079009), and the China Postdoctoral Science Foundation (2019M652649).

Data Availability Statement: The basic data used to support the findings of this study are included within the article and available from the corresponding author upon request.

Acknowledgments: The authors thank the anonymous reviewers for their detailed comments that helped to improve this article substantially. The first author is grateful for his wife, Yan Yan, for support and care.

Conflicts of Interest: The authors declare no conflict of interest.

References

1. Wu, Y.; Gao, Y.; Zhang, N.; Zhang, F. Simulation of spatially varying non-Gaussian and nonstationary seismic ground motions by the spectral representation method. *J. Eng. Mech.* **2018**, *144*, 04017143. [CrossRef]
2. Wu, Y.; Gao, Y. A modified spectral representation method to simulate non-Gaussian random vector process considering wave-passage effect. *Eng. Struct.* **2019**, *201*, 109587. [CrossRef]
3. Wu, Y.; Gao, Y.; Zhang, L.; Yang, J. How distribution characteristics of a soil property affect probabilistic foundation settlement—From the aspect of the first four statistical moments. *Can. Geotech. J.* **2020**, *57*, 595–607. [CrossRef]
4. Yao, E.; Miao, Y.; Wang, S.; Long, X. Simulation of fully nonstationary spatially variable ground motions on a canyon site. *Soil Dyn. Earthq. Eng.* **2018**, *115*, 198–204. [CrossRef]
5. Yao, E.; Wang, S.; Ruan, B.; Miao, Y.; Zhu, L. Numerical study on site response considering ground motion spatial variation. *Soil Dyn. Earthq. Eng.* **2019**, *127*, 105836. [CrossRef]
6. Yao, E.; Wang, S.; Miao, Y.; Ye, L.; Zhu, L. Simulation of fully non-stationary spatially varying ground motions considering nonlinear soil behavior. *Soil Dyn. Earthq. Eng.* **2020**, *129*, 105954. [CrossRef]

7. Fan, S.; Shi, Y.; Liu, C.; Li, W. Simulation of spatially varying seafloor ground motions with random seawater layer and complex terrain. *Soil Dyn. Earthq. Eng.* **2018**, *111*, 110–118. [CrossRef]
8. Bureau, G. New Considerations for Offshore Seismic Response Studies. In Proceedings of the Third U.S. National Conference on Earthquake Engineering, Vol. I, Charleston, SC, USA, 24–28 August 1986; pp. 789–795.
9. Feng, D.Y. *Theories and Applications of Seismic Wave*; Seismological Press: Beijing, China, 1988. (In Chinese)
10. Crouse, C.B.; Quilter, J. Seismic Hazard Analysis and Development of Design Spectra for Maul A Platform. In Proceedings of the Pacific Conference on Earthquake Engineering, Vol. III, Auckland, New Zealand, 20–23 November 1991; pp. 137–148.
11. Boore, D.M.; Smith, C.E. Analysis of earthquake recordings obtained from the Seafloor Earthquake Measurement System (SEMS) instruments deployed off the coast of southern California. *Bull. Seismol. Soc. Am.* **1999**, *89*, 260–274. [CrossRef]
12. Diao, H.; Hu, J.; Xie, L. Effect of seawater on incident plane P and SV waves at ocean bottom and engineering characteristics of offshore ground motion records off the coast of southern California, USA. *Earthq. Eng. Eng. Vib.* **2014**, *13*, 181–194. [CrossRef]
13. Li, C.; Hao, H.; Li, H.; Bi, K. Theoretical modeling and numerical simulation of seismic motions at seafloor. *Soil Dyn. Earthq. Eng.* **2015**, *77*, 220–225. [CrossRef]
14. Shi, Y.; Fan, S.; Liu, C. Theoretical modeling of spatially varying ground motions under ice-seawater interface and earthquake analysis of cable-stay bridges. *Soil Dyn. Earthq. Eng.* **2019**, *120*, 170–180. [CrossRef]
15. Zhang, D.Y.; Xie, W.C.; Pandey, M.D. Synthesis of spatially correlated ground motions at varying sites based on vector-valued seismic hazard deaggregation. *Soil Dyn. Earthq. Eng.* **2012**, *41*, 1–13. [CrossRef]
16. Li, C.; Hao, H.; Li, H.; Bi, K.; Chen, B. Modeling and Simulation of Spatially Correlated Ground Motions at Multiple Onshore and Offshore Sites. *J. Earthq. Eng.* **2017**, *21*, 359–383. [CrossRef]
17. Liu, G.; Liu, Y.; Feng, X.; Wang, D. Simulation of spatially variable seismic underground motions in saturated double-phase media with overlying water excited by SV-wave and difference from P-wave incidence. *Soil Dyn. Earthq. Eng.* **2019**, *123*, 144–161. [CrossRef]
18. He, Y.; Chen, X.; Liu, Z.; Yang, D.; Zhang, H. Simulation of Spatially Correlated Multipoint Ground Motions in a Saturated Alluvial Valley. *Shock. Vib.* **2021**, *2021*, 7056096. [CrossRef]
19. Bi, K.; Hao, H. Modelling and simulation of spatially varying earthquake ground motions at sites with varying conditions. *Probab. Eng. Mech.* **2012**, *29*, 92–104. [CrossRef]
20. Liang, J.; Liu, Z.; Huang, L.; Yang, G. The indirect boundary integral equation method for the broadband scattering of plane P, SV and Rayleigh waves by a hill topography. *Eng. Anal. Bound. Elem.* **2019**, *98*, 184–202. [CrossRef]
21. Huang, L.; Liu, Z.; Wu, C.; Liang, J. The scattering of plane P, SV waves by twin lining tunnels with imperfect interfaces embedded in an elastic half-space. *Tunn. Undergr. Sp. Technol.* **2019**, *85*, 319–330. [CrossRef]
22. Kiureghian, A.D. A coherency model for spatially varying ground motions. *Earthq. Eng. Struct. Dyn.* **1996**, *25*, 99–111. [CrossRef]
23. Lou, L.; Zerva, A. Effects of spatially variable ground motions on the seismic response of a skewed, multi-span, RC highway bridge. *Soil Dyn. Earthq. Eng.* **2005**, *25*, 729–740. [CrossRef]
24. Liao, S.; Zerva, A.; Stephenson, W.R. Seismic spatial coherency at a site with irregular subsurface topography. In Proceedings of the Sessions of Geo-Denver, Denver, CO, USA, 18–21 February 2007; Geotechnical Special Publication No. 170; pp. 1–10.
25. Bi, K.; Hao, H. Influence of irregular topography and random soil properties on coherency loss of spatial seismic ground motions. *Earthq. Eng. Struct. Dyn.* **2011**, *40*, 1045–1061. [CrossRef]
26. Wolf, J.P. Soil-structure-interaction analysis in time domain. *Nucl. Eng. Des.* **1988**, *111*, 381–393. [CrossRef]
27. Yang, J.; Sato, T. Interpretation of seismic vertical amplification observed at an array site. *Bull. Seismol. Soc. Am.* **2000**, *90*, 275–285. [CrossRef]
28. Clough, R.W.; Penzien, J. *Dynamics of Structures*, 2nd ed.; McGraw Hill: New York, NY, USA, 1993.
29. Sobczky, K. *Stochastic Wave Propagation*; Kluwer Academic Publishers: Alphen aan den Rijn, The Netherlands, 1991.

Disclaimer/Publisher's Note: The statements, opinions and data contained in all publications are solely those of the individual author(s) and contributor(s) and not of MDPI and/or the editor(s). MDPI and/or the editor(s) disclaim responsibility for any injury to people or property resulting from any ideas, methods, instructions or products referred to in the content.